Proceedings of the 4th International Conference on Computing and Data Science (CONF-CDS 2022)
DOI: 10.54254/2755-2721/2/20220562

Exploring The Use of Convolutional Neural Networks in UAV Based Rescue Missions

Xuande Andrew Shen[1]

[1]Berkshire School, Sheffield, MA, 01257, USA

andrewxdshen@gmail.com

Abstract. Multi-rotor based flight platforms, especially quadcopters and unmanned aerial vehicles (UAVs), and their embedded avionics have become emerging technologies in rescue operations. Due to the simplicity of mass production, as well as air superiority, rapid deployment and vertical take-off and landing (VTOL) capabilities, autonomous driving will be the next step in rescue operations. This project aims to explore the application of UAV combined with deep learning algorithm in drowning scenario. With the help of Betaflight, create an autonomous flight program that implements specific drowning rescue functions. Deep learning algorithms are critical to developing neural recognition networks for drowning individuals, with pre-programmed flight parameters eliminating the need for human interaction, human error to be precise. The core goal of the project is to improve the success rate of lifesaving solutions through the availability of this technology, a longer operating range than lifeguards, and shorter response times.

Keywords: UAVs, machine learning, convolution neural network, rescue missions

1. Introduction

On Father's Day, Sunday, June 20, 10-year-old Joscali Martinez tragically drowned off cape Conimicott Beach in Rhode Island. Local officials say Cardona Sanchez, 35, who was a stranger to the girl, jumped into the water to save her, only to get caught in the net. Two other people who witnessed the tragedy also tried to intervene but were taken to hospital. Unfortunately, due to strong currents and poor visibility, despite a search by several local agencies using helicopters and divers, they were unable to find the body [1].

One of the most dangerous dangers of water rescue is current, rip currents to be exact. The strong outflow of water and the channel at the bottom of the bed pose a hazard to inexperienced swimmer [2]. In the past year alone, the problem has been blamed for more than 4,000 deaths in the United States and more than 320,000 deaths a year worldwide [3,4]. In addition, nearby bystanders may end up in the hospital as a result of futile efforts to save these people. This is the first problem to be solved in this project.

The main reasons for the current low efficiency of drowning rescue are the prolonged time frame, dangerous conditions and the extensive requirements of first responders [5]. Once spotted, lifeguards activate the appropriate technology to save the person. Such a long process would quickly exceed the time frame for a person to be rescued, also known as the golden Age [6]. Drones can prove helpful in eliminating this process because of their constant vigilance and versatility. Drones can avoid dangerous water conditions, immediately identify individuals in distress, and provide lifesaving

DOI: 10.54254/2755-2721/2/20220562

equipment with a bird's eye view of the water. Therefore, the loss of life is minimized by reducing rescue time. In addition, due to lifeguard capacity and staffing limitations, an easy-to-use drone can increase the availability of lifesaving equipment and increase lifesaving range. In a recent survey, more than 88% of civilians expressed acceptance of the use of UAVs for Sea and Air Rescue (SAR) [7].

Naidoo et al. developed ai-based technology to process images taken by drones to detect injured people in the wilderness and provide assistance [2]. Qi et al. developed a drone for search and rescue operations after earthquakes. The system was successfully tested after the 2013 Lushan earthquake in China [8]. Lygouras et al. used a combination of computer vision algorithms and global navigation satellites to detect the heat in distress and dispatch rescuers [9].

2. Experimental methods

2.1. Identification System

Intelligent recognition systems must automatically recognize human actions that indicate struggling states and require other similar states. To achieve this level of recognition, the system will use machine learning to identify the behavior of workers and, through hundreds of other examples, improve its algorithms for determining whether individuals are working. Kumar et al. compared convolutional neural networks (ANN) with convolutional neural networks (CNN). Using data sets containing more than 14,855 photos, of which 1325 were identified with changeable expressions and background images, the results showed that CNN was superior to the accuracy of facial recognition and less in the period of Ann, that is, smaller training time [1]. Share et al. found that while thermal imaging proved to be the most accurate at identifying the presence of people, motion detection was best by establishing a pattern to identify drowning and non-drowning individuals.

2.2. Autopilot system

The flight controllers are designed to operate autonomously and perform rescue missions without human input. This is to increase response time while minimizing errors. The system features manual override of the case to monitor a specific situation by emergency personnel. Autonomous flight requires intercepting the receiver's signal lines so that the receiver can be run through an Arduino board and then connected to the flight controller. Connect two power cables to power both the motherboard and the receiver via the drone battery. This hardware setup allows a pre-planned set of pulse position modulation (PPM) signals, known as the autonomous flight plan, to be sent from the Arduino as a receiver to the flight controller. In addition, two signal lines from the GPS were reconnected to the Arduino board to provide telemetry for autonomous flight.

2.3. Bed for drone flight

The material selection is limited to 3D-printed materials to maintain the drone's essential value for simple mass production and maintenance. While most drones use carbon fiber infused polycarbonate as the primary material, the cost and equipment required to manufacture cF-PCS in 3D printers are low-cost. Table 1 provides a detailed overview of the theoretical materials available. Polylactic acid (PLA) was chosen over acrylonitrile butadiene styrene (ABS) and polyethylene terephthalate (PETG), two other popular plastics, because of their strength, flexibility and weight.

DOI: 10.54254/2755-2721/2/20220562

Table 1. Filament Data

	PLA	ABS	PETG	CF PC
Recycled Content	55%	65%	67%	42%
E-modulus	3120 MPa	1900 MPa	2020 MPa	2300 MPa
Tensile Strength at Yield	38 MPa	44 MPa	50.4 MPa	57 MPa
Strain at Break	19.5%	9%	22.7%	370%
Yield Strain	4.8%	2.8%	5.9%	6%
Flexural Strength	N/A	56 MPa	69 MPa	102 MPa

3. Software system development

3.1. Convolutional intelligent recognition system

A TypeScript library is used to provide the basis for neural networks. In addition to the original neural network framework, A represents the instruction code for identifying drowning persons. A basic set of images of all individuals is used to establish the primary target of the recognition software. The program requests the data captured by the camera and stores the requested data in the results for later use. From the results of the image data, the program retrieves the desired results. This can be done by identifying the X center of the ID1 box in the data. Process the results of the image from the center box and process the parameters of the image. Retrieves and compares setting parameters from the raw image cache to determine a partial match. The last section ensures that the program keeps iterating through the NTH data result box, building its repository.

The parameters that determine a person's drowning and non-drowning status fall into four categories. The first parameter identifies the white area around the individual in the ID1 box. The number of pixels represents the paint and is equal to the degree of movement, which could mean drowning. The second parameter defines the size of a person's mouth. Similarly, pixels within the ID1 box are analyzed to determine how much a person craves oxygen. Third, pixel movements of individual arms are compared in multiple images to determine movement speed. This is used to judge whether a person is in a desperate, dangerous situation. The fourth parameter is similar to the third but may represent a loss of consciousness compared to lack of movement. In cases where a secure call takes precedence over a false call, identification is based on matching two of the four parameters that would prevent a rescue operation.

Further requirements of the system include signal output in the case of parameter matching. To this end, output 10 on the motherboard is encoded into the program to provide a short burst of power to turn the servo motor connected to pin 10. The system is designed to trigger the release mechanism of the lifejacket deployment system once an individual is identified. As the drone patrols the designated area, the on-board camera will constantly provide images via software to look for people in distress. Once the program determines that a person meets the program's requirements, the drone above the person releases the life jacket.

3.2. Autonomous flight

To generate PPM, show the digital pins on the Arduino fluctuating from high to low in the required time. The first iteration of the code, sets the pin output to HIGH, waits for 500 μs, and sets the result to LOW by writing an impulse function. Pulse timing is used to complete the precise timing of pulses. By economizing time in microseconds, you can generate a while loop until the difference between the microseconds and the start time of the save is 500 μs. A second function, Gen PPC, is written to pulse at the appropriate time interval. Here you write a for loop that waits through each pulse and according to the desired channel value using the same method described above. Finally, the last extended delay signal sends a new data frame. Using Betaflight, you can see that the transactions on the slider are

DOI: 10.54254/2755-2721/2/20220562

about the same as expected but are significantly unstable. The fluctuation range is more than $\pm 100\ \mu s$. The Pulse function was removed, and the code was inserted into gen PPC when needed to minimize the jump time between tasks in the code. This works at the minimum for each channel, but channel 6 has a bigger error when all six channels are set to a maximum of 2000. Again, this function was changed to form the current time micros directly before each wait period. Errors are not generated via the pulse and negatively affect channels. Through combination, the values of all six channels fluctuate less than 10 μs, which is not consummate, but enough to ignore the impacts of flight.

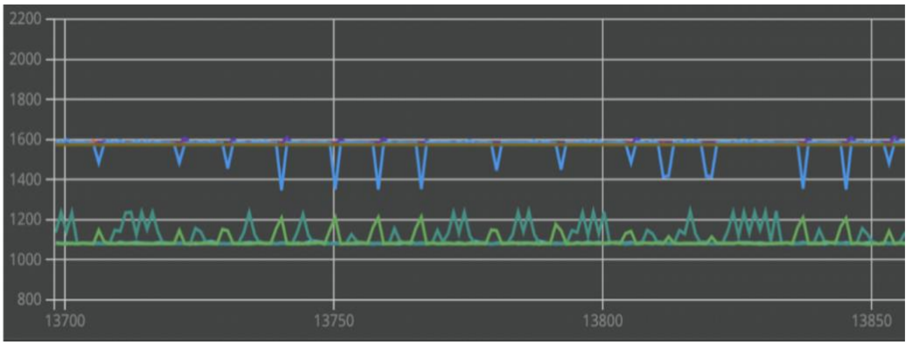

Figure 1. Pulse position modulation interval at 17500 μs at steady condition

The reason for this could be a fraction of the time it takes to run the code, as well as a flaw in the microprocessor's own functionality. Micros has a resolution of 4 μs, so additional microseconds can be added or subtracted depending on the start time of the pause, resulting in slight instability of the Gen PPC function [10].

To maximize the effectiveness of the GEN PPC function, pauses at the end of the frame need to be minimized. While longer rest times result in durable values, there is a longer delay between sending commands and receiving them by flight controllers. Figure 1 shows the test with a pause time of 17500 μs.

In this case, the maximum deviation under the stable condition is 200. It is the state when the steady-state transmitter is in the well-balanced position. Roll, yaw and pitch should be 1500, and throttle and two auxiliary channels should be 1000. These auxiliary channels correspond to the switches on the transmitter. In this case, the two auxiliary channels and yaw fluctuate the most. In further research, channel 3 and channel 4 are switched in the slider of Betaflight, which means that these three unstable channels are the last three in the frame. Because even in the other microS calls described above, errors will occur. When the most unstable state is found, a maximum condition is also tested. All values of here are set to 2000, except Aux 1, 1000. Figure 1 shows the top test% with the same pause length.

This experimental condition was found through repeated experiments. As shown in Fig.2, compared with the situation in Fig.1, very inconsistent results are produced-under a specific pause value, the maximum test condition produces exciting results. Except for small peaks, these values are stable enough to rise. Whereas they do not represent what is needed. Aux 1 is 1300 when it should be 1000; When x = 2000, x = 1000. Roll, pitch and yaw are close to 1700, when they should all be 2000,as shown in Fig.3.

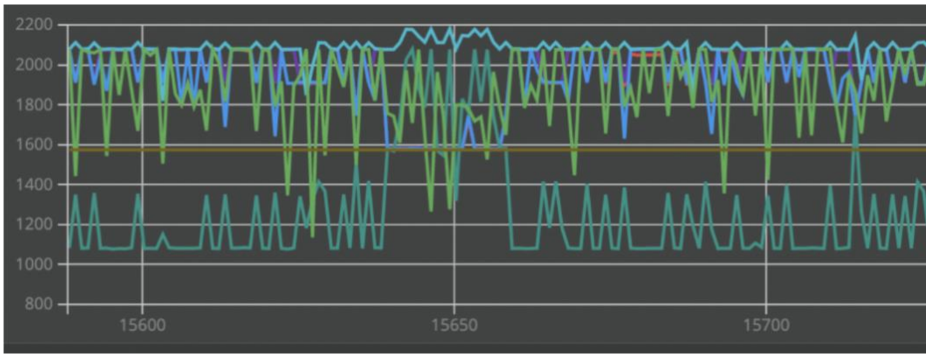

Figure 2. Pulse position modulation interval at 17500 μs at the maximum condition

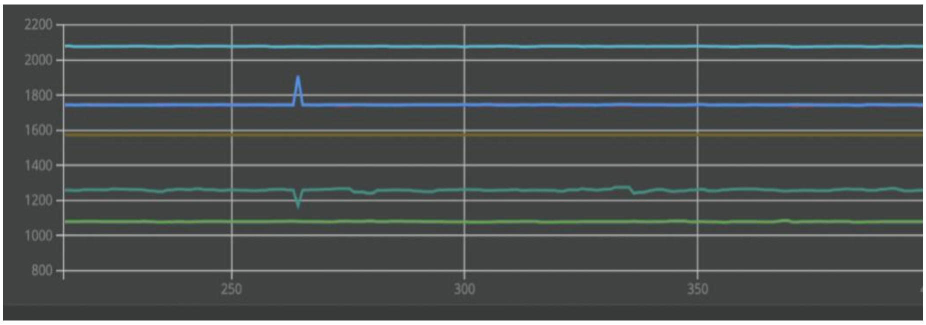

Figure 3. Pulse position modulation interval at 20000 μs at the maximum condition

At 35,000 μs, the worth of all channels in the PPM signal remain stable, regardless of the conditions under which they are placed. This was reconfirmed during the next two pause times, confirming that the threshold pause was less than 35,000. Sufficient information is obtained to encode the autonomous flight mode and control switch by employing the library to assist read the input signal from the receiver. Two auxiliary channels are set up as two buttons on the transmitter. Auxiliary 2 is 1000 or 2000 and is used for armed drone flying Auxiliary 1 controls automatic and manual flight with three positions, 1000,1500 and 2000. The main iteration part of the Arduino code (void loop) reads the PPM signal from the receiver and consists of a series of logical statements that end with a call to the Gen PPC function. The reader encodes an array of channel values passed into the PPM signal, and these values change or do not change depending on the logical statement. Finally, Gen PPC creates PPM signals for the flight controller based on these array values. The first logical statement switches the code from manual to automatic. Finally, there exists statement that tests whether the current levelThrot value is not equal to zero. If the value is not equal to zero, the mode is automatic; if value is manual, the mode is skipped [11].

4. Hardware design

4.1. The arm

For versatility, motor mounting holes need to be flexible on hand to supply the motor. Motor sizes range from 2204(mount mode 1616) to 2212(mount mode 1919) for optimal thrust-to-weight ratio for SAR. Aerodynamic design is also critical in the high wind speed and high-speed requirements of coastal environments. The bottom of the arm consists of a rounded semi-cylinder to support the application. The upper part of the peninsula is formed by a trapezoidal structure to provide structural support. To create more aerodynamic handling, a further design change is the upsloping arm structure, which will allow a smoother descent for individuals in distress.

Use a common design construct. The next steps involved reducing weight while maintaining the structural integrity of the arm. This involves hollowing out an area within the component without significantly reducing the strength. The first step is to punch holes in the structure. Due to the

DOI: 10.54254/2755-2721/2/20220562

limitations of SLS and FDM 3D printing technology, the minimum width of one side must be at least 8mm. The width of each side is 10mm and the error space is 2mm(FIG. 4b). In addition, the pillar uses a honeycomb interior filling design to reduce overall weight by 80%, while adding vertical bracing to improve durability during takeoff and landing.

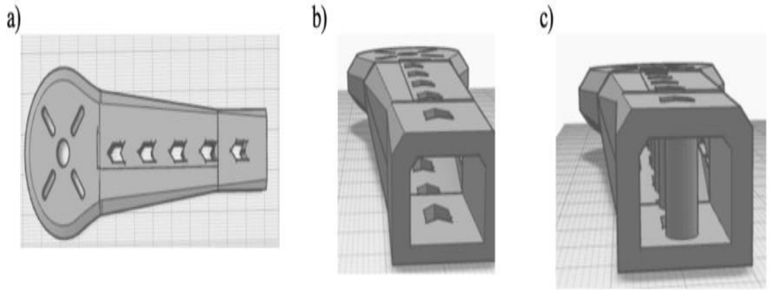

Figure 4. Drone arm weight reduction

4.2. Arm - chassis connection and landing gear legs

For mounting connections, requirements include uniform distribution of pressure, rigid construction, and easy commercial replication. M3 bolts instead of M2 bolts were used to increase the size, and the weight increase was not obvious. The larger size indicates a more even distribution of pressure across the connector, rather than the accumulation of pressure during extreme movements at a single stress point. For landings, durability is key to ensuring operational life. The triangle is a basic structure to create a strong base to absorb shocks without breaking. To save weight, one side of the pyramid was turned upside down. A number of minor cosmetic changes were made to ensure a smoother landing, including a vertex flattening.

After all the components were assembled within the Fusion 360, the final cosmetic changes were made to the entire arm. The results shown in Figure 5 show a smooth arm with aerodynamic forms and important connection points to the frame. Aerodynamics and stress testing allow for further modifications and improvements to the design.

4.3. UAV on chassis

Eid et al. found that the pressure distribution was greatest on the outer surface of the lower chassis, where the wind blows, and then smallest upper chassis. In addition, due to the lower width from the edge of the hole to the edge of the frame [12], the pressure around the hole created in the design will have a high value. As a result, the center chassis is reinforced with additional support to offset the higher pressures. The chassis at the top is designed with a basic square attached to a slender hexagon that rotates 45 degrees at the corners of the arm connections (Figure 6A). Thermal vents were added to ensure constant air flow to the flight controller and processor as natural heat sinks (Figure 6b). Two entry channels are added to the sides of the case, and motor wires will enter connected to ESC cables for management and security. The arm connection is inserted into the bottom plate for reference. In addition, bolt holes were added to enhance bolt stability under turbulent conditions (FIG. 6d).

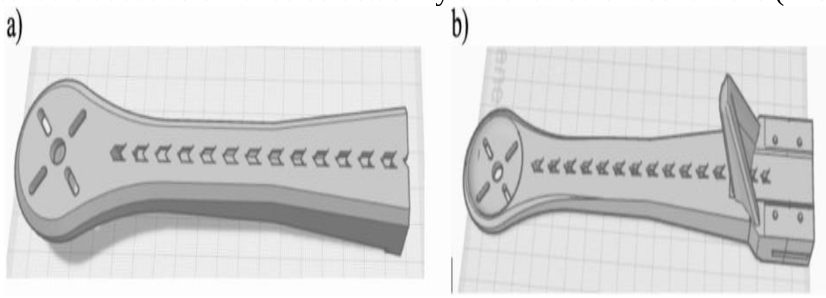

Figure 5. Complete drone arm

DOI: 10.54254/2755-2721/2/20220562

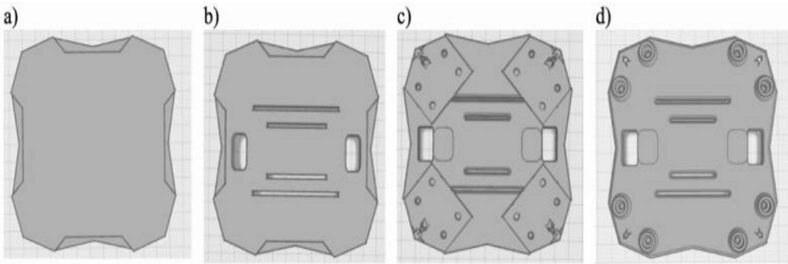

Figure 6. Top frame

4.4. Drone bottom chassis

The bottom chassis has the same basic construction, with four additional 4 handles on each side, and the life jacket ejection system can be connected (FIG. 7a). As mentioned earlier, the mounting holes for flight controllers will change to accommodate accessibility and supply. Therefore, linear grooves were made to accommodate 30 x 30 and 25 x 5 flight controllers, rather than a fixed mounting platform. These rails are also used as basic radiators.

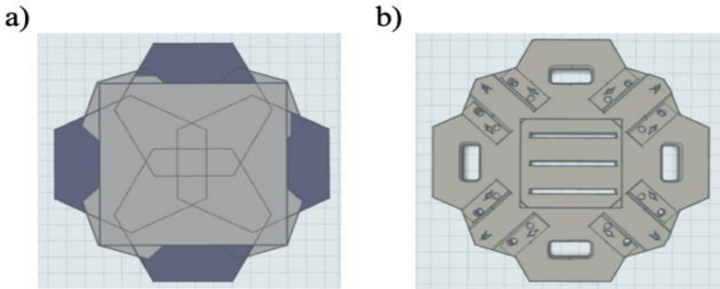

Figure 7. Bottom frame

4.5. Life jackets drop system

The rescue system is a simple use of servo motor pull needle. A servo motor capable of rotating 90 degrees will be attached to the bottom of the drone. A separate cylinder with two holes on opposite sides is also attached to the bottom chassis. The arm of the motor will be connected to a needle that passes through the cylinder to hold it in position. When triggered, the servo motor rotates, pulling the plug out of the cylinder and dropping the package from the hook (FIG. 8).

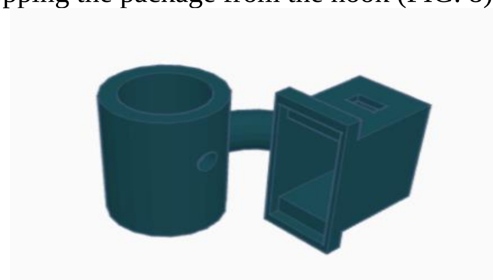

Figure 8. Life Vest Ejection Device

5. Results

As shown in Figure 9, the pressure distribution on the outer surface of the lower chassis is greatest, where it is impacted by the wind, while the pressure distribution on the outer surface of the upper chassis is minimal. In addition, due to the lower width from the edge of the hole to the edge of the frame, the pressure around the hole created in the design will have a high value. This limitation was due to size limitations, but additional support in the middle chassis was placed to reduce stress in these areas.

DOI: 10.54254/2755-2721/2/20220562

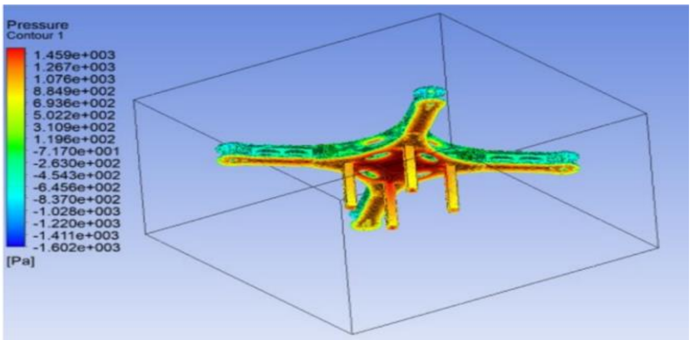

Figure 9. Pressure distribution over hovering design (bottom view)

One of the key domains of frame design is to determine the lift coefficient of the frame. Calculate full weight of the design from the lift and thrust generated by the engine, including assuming that takeoff is a pure vertical motion with no tilt. The wind direction is vertical, the horizontal axis resistance can be ignored, and the stable wind speed is 30m /s. The lift coefficient calculated by CFD is 0.23.

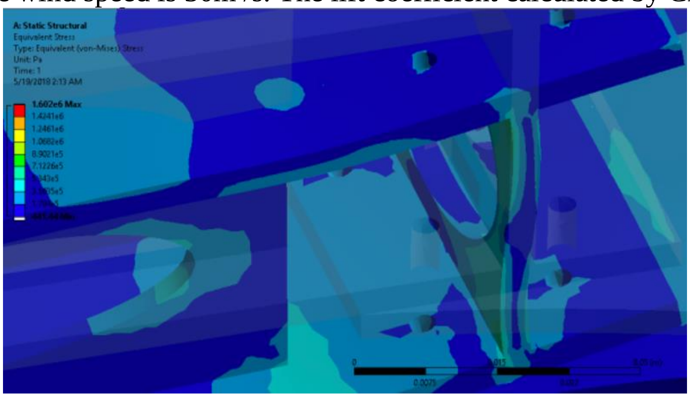

Figure 10. Von Mises stresses, Final Design

The gross deformation and equivalent stress inaccuracies obtained in the verification of the results are approximately 15%, which is due to the approximation of the UAV chassis application. The chassis of UAV is fixed by cantilever beam, which is connected and fixed from the side of the frame. However, the maximum stress obtained is at the lower edge of the relationship between the UAV chassis and the frame (Figure 10). A small bracket supports the connection between the UAV chassis and the frame, reducing stress on important components and transferring stress to the bracket. In this way, any failure can occur on a stand that can be easily replaced at the lowest cost.

Whereas the maximum deformation experienced by the design under static load is considered to be minimal as it is less than 0.3 mm (FIG. 10). These results ensure that the selected material (PLA) can withstand the load of the component at rest. The resulting deformation is low considering the weights of the elements acting on it. In addition, the deformation is further reduced by the rigid fixing bracket.

Furthermore, testing from multiple experimental flights made it possible to derive operational estimates from the data received. Different experimental iterations included scenarios with and without life jackets, including round-trip trips. In addition, the test lasted five days and included different airspeeds taking into account other atmospheric conditions for coastal terrain. The flight time with no standard drag and corresponding speed. At 33 kilometers per hour, the flight time without standard pain is about 16 minutes.

A full system test was performed on the drone to determine the speed of the entire platform relative to the lifeguard. The purpose of the test was to determine whether the initial goals of a drone with a shorter response time and a greater operational range than lifeguards were met, all in the interest of saving lives. A radar gun is used to determine the drone's speed at different stages of flight. The first image on the left of Figure 11 is the initial phase of the flight after takeoff. The radar gun showed a

DOI: 10.54254/2755-2721/2/20220562

speed of 12.3 km/h. The second image shows the drone entering a designated patrol area with preset autopilot parameters. The top speed is 28.2 kilometers per hour. Figure 3 shows UAVs in patrol operations. To ensure fast and accurate scanning, the drone is programmed to travel at a speed of 24 km/h. Due to the wind conditions at the site during the test, the drone flew at a speed of 24.8 km/h. By comparison, the occupational health standard for lifeguards is a paddle speed of 1.38 m/s. That means they should be able to run at speeds of 82.8 m/min and 4,968 m/h. At that rate, the drone is far faster than the lifeguard. Thus, this shows that the UAV is superior to the lifeguard in terms of speed and lifesaving capability, achieving the original engineering and program objectives.

Figure 11. Speed test of complete platform (with auto-inflatable green life vest attached)

6. Conclusion

This paper discusses the integration of convolutional intelligent system and multi-rotor aircraft for drowning recognition. The production and programming of the entire project indicates a relatively simple mass production process. This is critical to the project because its core objectives are to make life-saving tools more accessible, eliminate human error and response times, and successfully deliver assistance when needed. With this technology, the risk to lifeguards and individuals in the water is greatly reduced. In addition, 3D manufacturing in conjunction with the quadcopter platform maximizes the success rate based on stability, speed, deployment time and operational range.

References

[1] Zhiqiang Chen. (2012). Defect diagnosis of Rotating Machinery Bearing based on convolutional Neural Network. Chinese Journal of Scientific Instrument, 32(1): 1-7. https://doi.org/10.1109/TIM.2021.3055802

[2] Naidoo Y Stopforth, R, & Bright, G (no date). Development of an UNMANNED aerial vehicle for search and rescue. The IEEE explore. https://doi.org/10.1109/AFRCON.2011.6072032

[3] Ijeh, A. C., & Curran, K.(2021). Criminal science and digital Forensics: a holistic perspective. CRC Press.

[4] Feraru v. Anderson, R. E. & Boukas large intestine (no date). To develop an automatic search and rescue system based on UAV to assist search and rescue personnel overboard accidents. IEEE Xplore.

[5] Zhiqiang Wang, Zhiqiang Liu, Zhiqiang Liu, Zhiqiang Xu (2018). Additive Manufacturing (3D printing): A review of materials, methods, applications, and challenges. Composites Part B: Engineering, 143,172-196. https://doi.org/10.1016/j.compositesb.2018.02.012

[6] Hiebert B., Nouvet, E., Jeyabalan, V., & Donelle, L.(2020). Use of unmanned aerial vehicles in Healthcare and health-related Services in North America: a scoping review. Unmanned Aircraft,4(3),30. https://doi.org/10.3390/drones4030030

[7] Liu Zhiqiang, Liu Zhiqiang. (2014). Driverless cars are addressing new applications in healthcare, agriculture, as well as the military and security as they become smaller and smarter. Industrial Robot, 41(1), 82-86. https://doi.org/10.1108/IR-03-2013-410

[8] J. Qi, Song, D, Shang,H. N hua C wu C qi X , and Han Nationality, J. (2015). Search and rescue rotorcraft UAV and its application in Lushan ms7.0 earthquake. Chinese Journal of Robotics, 33(3), 290-321. https://doi.org/10.1002/rob.21615

[9] Lygouras, E., Santavas, N., Taitzoglou, A., Tarchanidis, K., Mitropoulos, A. And Gasteratos, a. (2019). Unsupervised human detection using embedded vision systems on a fully autonomous UAV for search and rescue operations. Sensor,19(16),3542. https://doi.org/10.3390/s19163542

[10] Ginsberg, S.ND. Autonomous Drone: Modified a DIY drone kit for autonomous flight. Wash the university. https://doi.org/10.7936/tb5e-8r31

[11] Anderson, i. (2017). Mechanical properties of samples 3D printed with primary and regenerated polylactic acid. 3D Printing and Additive Manufacturing, 4(2), 110-115. https://doi.org/10.1089/3dp.2016.0054

[12] Ajgaonkar, K., Khanolkar, S., Rodrigues, J., Shilker, E., Borkar, P., & Braz, E.(North Dakota) to develop a lifeguard assisted UAV for coastal search and rescue. IEEE Xplore. https://doi.org/10.1109/IEEECONF38699.2020.9389382